Editorial Manager(tm) for International Journal of Fracture
Manuscript Draft

Manuscript Number:

Title: Single Fiber and Multifiber Unit Cell Analysis of Strength and Cracking of Unidirectional Composites

Article Type: Original Research

Section/Category:

Keywords: Micromechanical modelling; Fiber reinforced composites; Damage evolution; Cohesive elements; Finite element method

Corresponding Author: Dr. Dr. habil. Leon L. Mishnaevsky Jr.,

Corresponding Author's Institution: Risø National Laboratory,

First Author: Huaiwen Wang, Professor

Order of Authors: Huaiwen Wang, Professor; Hongwei Zhou, Professor; Leon L. Mishnaevsky Jr.; Povl Brøndsted, Dr. ; Lina Wang

Manuscript Region of Origin:

Abstract: Numerical simulations of damage evolution in composites reinforced with single and multifibers are presented. Several types of unit cell models are considered: single fiber unit cell, multiple fiber unit cells with one and several damageable sections per fibers, unit cells with homogeneous and inhomogeneous interfaces, etc. Two numerical damage models, cohesive elements, and damageable layers are employed for the simulation of the damage evolution in single fiber and multi fiber unit cells. The two modelling approaches were compared and lead to the very close results. Competition among the different damageable parts in composites (matrix cracks, fiber/matrix interface damage and fiber fracture) was observed in the simulations. The strength of

interface begins to influence the deformation behaviour of the cell only after the fiber is broken. In this case, the higher interface layer strength leads to the higher stiffness of the damaged material. The damage in the composites begins by fiber breakage, which causes the interface damage, followed by matrix cracking.

Single Fiber and Multifiber Unit Cell Analysis of Strength and Cracking of Unidirectional Composites

Huaiwen Wang [a, b*], Hongwei Zhou [b], Leon Mishnaevsky Jr.[c], Povl Brøndsted [c], Lina Wang [b]

[a] School of Mechanical Engineering, Tianjin University of Commerce, Tianjin 300134, China
[b] Institute of Rock Mechanics and Fractal, China University of Mining and Technology (Beijing), Beijing 100083, China
[c] Risø DTU National Laboratory for Sustainable Energy, Technical University of Denmark, AFM-228, P.O. Box 49, Frederiksborgvej 399, DK-4000 Roskilde, Denmark

Abstract: Numerical simulations of damage evolution in composites reinforced with single and multifibers are presented. Several types of unit cell models are considered: single fiber unit cell, multiple fiber unit cells with one and several damageable sections per fibers, unit cells with homogeneous and inhomogeneous interfaces, etc. Two numerical damage models, cohesive elements, and damageable layers are employed for the simulation of the damage evolution in single fiber and multi fiber unit cells. The two modelling approaches were compared and lead to the very close results. Competition among the different damageable parts in composites (matrix cracks, fiber/matrix interface damage and fiber fracture) was observed in the simulations. The strength of interface begins to influence the deformation behaviour of the cell only after the fiber is broken. In this case, the higher interface layer strength leads to the higher stiffness of the damaged material. The damage in the composites begins by fiber breakage, which causes the interface damage, followed by matrix cracking.

Keywords: Micromechanical modelling; Fiber reinforced composites; Damage evolution; Cohesive elements; Finite element method

1. Introduction

Fiber reinforced composites find wide applications in aerospace and marine industry, wind power, automobile, civil engineering, national defence, etc., due to their high strength, low weight and high toughness. Research on fiber reinforced composites has attracted much attention in mechanics and materials science fields, and led to many publications with new information of fiber reinforced composites in wide fields.

In practice, components made from fiber reinforced composites may eventually fail because of pre-existing defects such as micro-cracks, voids and interface debonding. The reliability of the components from fiber reinforced composites may be predicted and eventually increased on the basis of the analysis of the effect of the composite microstructure on the strength and damage evolution. Such an analysis can be carried out in the framework of computational experiments [1-3].

In order to model the damage and failure of fiber reinforced composites under mechanical load, several modelling approaches are employed [1]: the shear lag and other analytical models, used to analyze the load transfer and multiple cracking in composites [4-7], fiber bundle model [8-9],

* *E-mail adress*: leon.mishnaevsky@risoe.dk

fracture mechanics-based models [10-12], numerical continuum mechanical models [1-3, 13-18]. The numerical continuum mechanical models, usually finite element models, allow the incorporation of many different features of the nonlinear material behaviors and the analysis of the interaction of available and evolving microstructural elements [1-3, 13].

In this work, we used numerical continuum mechanical models to simulate the damage evolution, interaction between different damage mechanisms, and the effect of the phase and interface properties in unidirectional glass fiber reinforced composites under tension load. Results with different modelling, cohesive elements modelling and damageable layer + element weakening technique modelling, were compared. The results of the simulation are expected to provide some parameters for the optimal design of these glass fiber reinforced composites.

2. Generation of Unit Cell Models of Composite with Damageable Elements

2.1. 3D Unit Cells with Single and Multiple Fibers

A number of unit cell models of composites were generated with the use of the program code "Meso3DFiber" [1-3]. The program generates a command file for the commercial FE pro- and post-processing software MSC/PATRAN©, which produces a 3D unit cell model of composite with pre-defined parameters. The finite element meshes are generated by sweeping the corresponding 2D meshes on the surface of the microstructure models. The program "Meso3DFiber" is described in more details elsewhere [1-3].

Several unit cell models with single fiber and many fibers are shown in Fig. 1. The unit cells were subject to a uniaxial tensile displacement loading along the axis of fiber (*Z* axis direction). The boundary conditions of this simulation were as follows: all degree of freedoms of point (0, 0, 0) was fixed, the 3rd degree of freedom of bottom surface with coordinate z=0 was restricted, and the 1st degree of freedom of line with x=0 and z=0 was restricted. Three-dimensional 6-node linear triangular prism element C3D6 was employed in this simulation for fiber, interface layer and matrix. The volume content of fiber is 4% in single-fiber model.

The epoxy matrix composite reinforced with glass fibers was studied in this paper. Table 1 shows the properties of the phases used in the simulations. The data were taken from [2, 19-22].

After the model is created in PATRAN©, the input file for FE commercial code ABAQUS© will be generated. The simulations were carried out with ABAQUS©/STANDARD.

Table 1. Properties of the phases used in the simulations [2, 19-22]

	Young modulus, GPa	**Poisson ratio**	**Failure criterion, MPa**
Fiber	72	0.26	Single-fiber modelling: Constant fiber strength with different value in different model. Multi-fiber modelling: Weibull distribution with parameters σ_0=929.8MPa and m=2.55.
Matrix	3.79	0.37	67 MPa
Interface	37.9	0.37	Different value in different model.

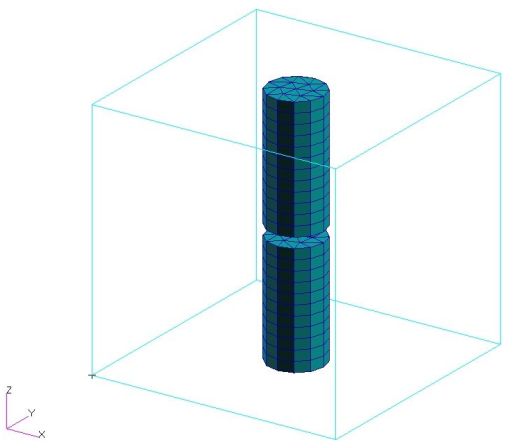

(a)

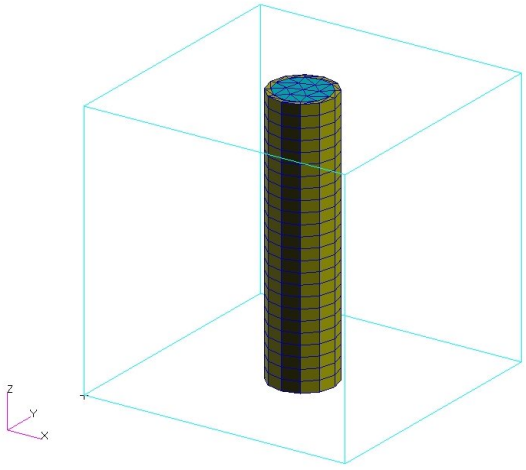

(b)

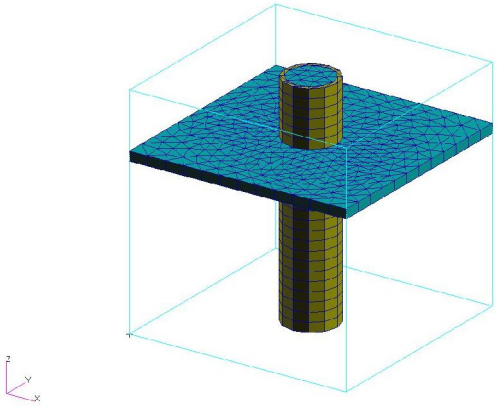

(c)

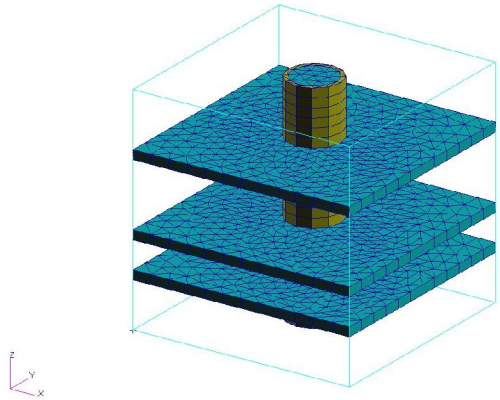

(d)

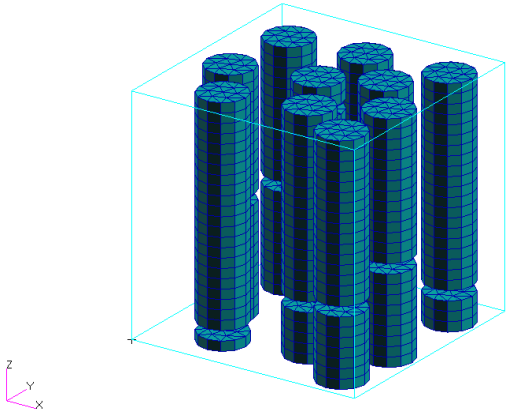

(e)

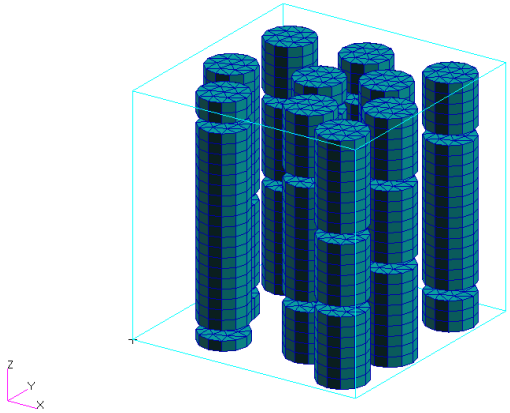

(f)

Figure 1. FE microstructural models used in this study: (a) single-fiber model with one damageable layer in fiber, (b) single-fiber model with one damageable layer in fiber and fiber/matrix interface layer, (c) single-fiber model with one damageable layer in fiber, fiber/matrix interface and a damageable layer in the matrix, (d) single-fiber model with one damageable layer in fiber, one fiber/matrix interface and three damageable layers in the matrix, (e) multi-fiber model with one damageable layer per fiber, (f) multi-fiber model with two damageable layers per fiber

2.2 Techniques of modelling damage: damageable layer + element weakening techniques versus cohesive elements

In order to model breaking of fibers, two modelling techniques were employed: an approach based on the introducing damageable layer and the element weakening techniques, and the cohesive element model.

The damageable layers were introduced into sections of fibers, following the idea by Gonzalez and LLorca [23]. The damageable layers have the same mechanical properties as the rest of the fiber. The damage evolution in the damageable layers was modelled by using the finite element weakening method [1-3]. In the framework of this method, the stiffness of a finite element is reduced if a stress or a damage parameter in the element or a nodal point exceeds some critical level. This conditions was realised in the ABAQUS© subroutines User Defined Field [1-3, 24-25]. The subroutine checks whether the element failed or not according to the properties of the damageable layer. A detailed description of this process can be referred in [1-3].

A similar concept was used to simulate the matrix cracking and interface damage of composites. Following the idea from [1-3], we modelled the interface damage as a weakening of finite elements in a special "interface layer". The interface was presented therefore as a special thin layer between the fiber and matrix. The damage evolution in this layer was modelled using the subroutine USDFLD as well.

The modelling technique described above was compared with the cohesive elements modelling. Cohesive elements were placed in the damageable layers of fibers, matrix or interfaces. Three-dimensional 6-node linear triangular prism cohesive elements COH3D6 or three-dimensional 8-node linear brick cohesive elements COH3D8 were used in the cohesive layers. The cohesive elements connected to other elements by sharing modes.

The stiffness of the cohesive elements was calculated as Young modulus divided by the thickness of cohesive element, and was 172 GPa. The maximum nominal stress traction-interaction failure criterion was selected for the damage initiation in the cohesive elements, and the energy-based damage evolution law is selected for damage propagation.

2.3 Determination of the damage criteria of the cohesive elements

Further, the simulations of the damage evolution in the microstructures with different cohesive elements damage initiation stress have been carried out, using the single fiber unit cell, shown in Fig. 1(a). Several levels of the damage initiation stress of cohesive elements have been taken: 100, 200, 300, 400, 500, 600, 700, 800, 900, 1000, 1100, 1200, 1250 and 1324MPa (the last values

corresponds to the critical stress for fiber given in Table 1). The damage dissipation energy ALLDMD for whole model plotted versus damage initiation stress is shown in Fig. 2.

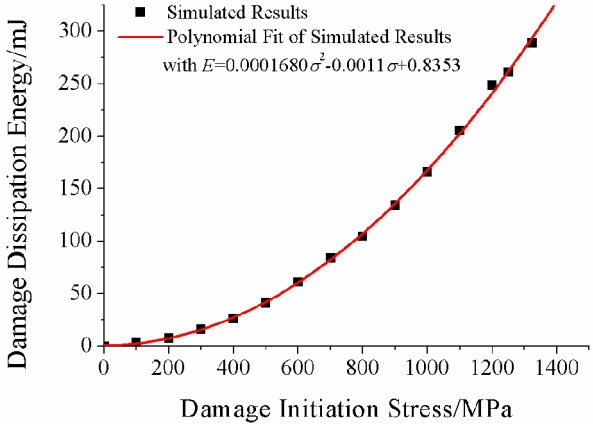

Fig. 2. Damage dissipation energy-damage initiation stress curve

Fig. 2 shows that the relation between the damage dissipation energy and the strength of the cohesive layer is obviously not linear. We fit the simulated results with quadratic polynomial function by the least square method. The relation between damage dissipation energy and damage initiation stress can be expressed by:

$$E = 0.0001680\sigma^2 - 0.0011\sigma + 0.8353 \quad (1)$$

4. Computational experiments: Single-fiber unit cell models

In this chapter, the damage evolution in 3D single-fiber unit cell models is investigated. In so doing, the damageable layer + element weakening approach and cohesive elements modelling are used and compared.

4.1 Single fiber unit cell: damageable layer versus cohesive element model

A single-fiber FE unit cell model with one damageable layer in fiber was considered here (see Fig. 1(a)). The damage evolution was modelled using two approaches: the weakening element layer model and the cohesive elements. Stress-strain and strain energy-strain curves as well as stress and strain distributions in the models were determined. Figures 3 and 4 show nominal stress-strain curves and strain energy-strain curve of the unit cell model, respectively. The maximal principals stress distributions before and after the fiber failure are shown in Fig. 5 and Fig. 6.

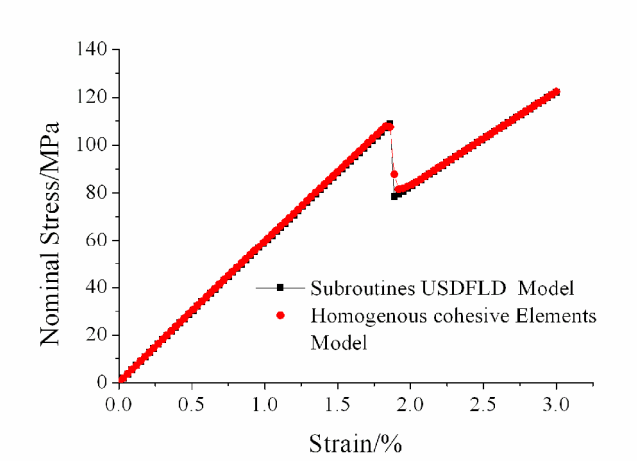

Fig. 3 Nominal stress-strain curve of the cell models with different model

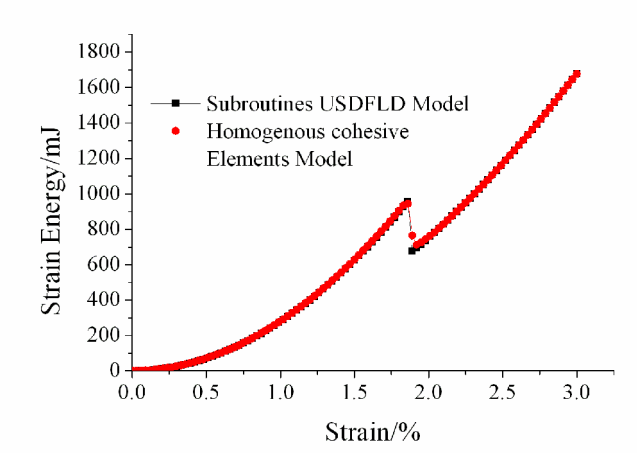

Fig. 4 Strain energy-strain curve of the cell models with different modelling

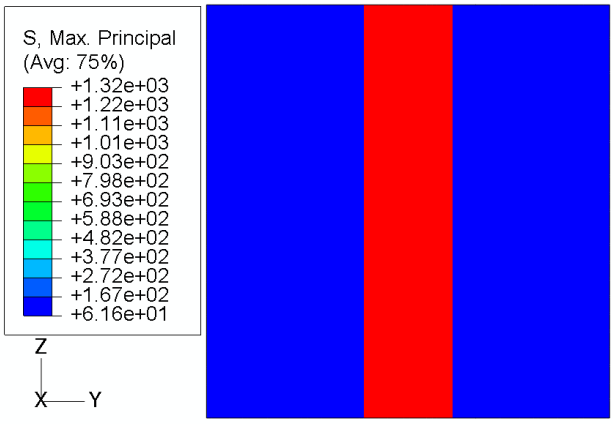

(a) Just before damage initiation (ε=1.86%)

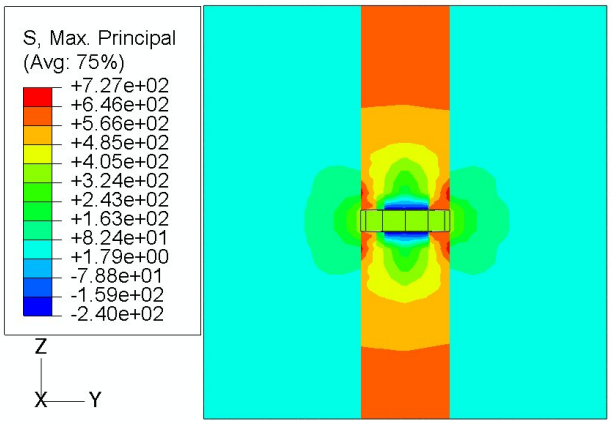

(b) Just after damage completed (ε= 1.89%)

Fig. 5 Maximal principal stress distribution in damage evolution process (Damageable layer model)

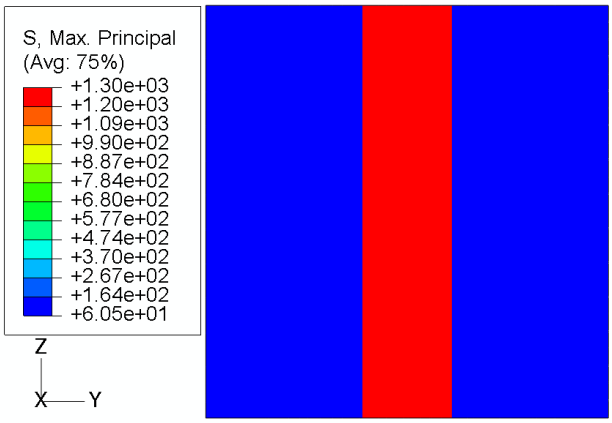

(a) before damage initiation (ε=1.86%)

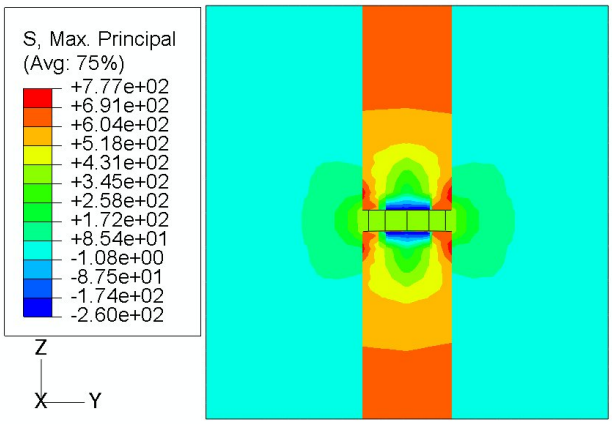

(b)Just after fiber is broken (ε=2.07%)

Fig. 6 Maximal principal stress distribution in damage evolution process (Cohesive elements model)

From Fig. 3, one can see that the stiffness of the composite decrease at ε=1.86% for both models. However, in the case of damageable layer model, the maximum principal stress in the glass

fiber decreases suddenly from 1.32×10^3MPa to 7.27×10^3MPa, as shown in Fig. 5. In the case of the cohesive elements model, the maximum principal stress in glass fiber decreased gradually from 1.30×10^3MPa to 7.77×10^3MPa (see Fig. 6). Simultaneously, the strain energy of the models decreases, as shown in Fig. 4.

From Figures 3-6, one can see that both the considered models give very similar results, both as related to the overall response, failure point and the stress distribution. However, the stress evolution due to the fiber failure is different for the two considered damage models: the stress decrease suddenly in the case of the damageable layer model, and gradually in the case of the cohesive elements model.

4.1.2 Single fiber cell: Effect of local inhomogeneity of the damageable fiber material

In order to take into account the local, nanoscale heterogeneity of fiber material, we introduce the variability of element properties in the cohesive layer. An element at the edge of the cohesive elements layer was assigned a lower damage initiation strength (here, 600MPa was employed while other elements with 1200MPa).

The evolution processes of the damage variable SDEG (scalar stiffness degradation at integration points) for homogeneous cohesive layer model and inhomogeneous cohesive elements layer model are shown in Fig. 7 and Fig. 8. The nominal stress vs. strain curves and strain energy vs. strain curves are shown in Fig. 9 and Fig 10.

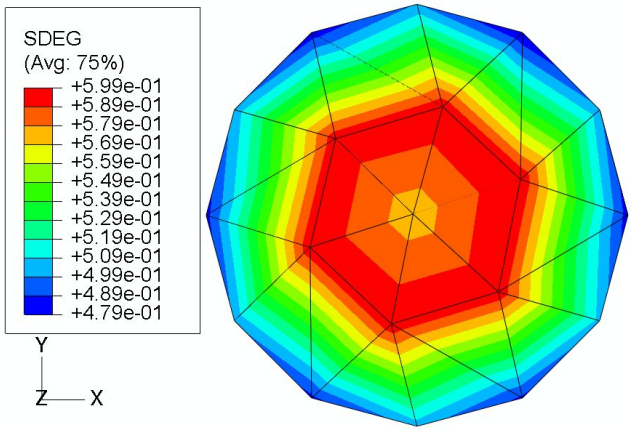

(a) ε=1.71%

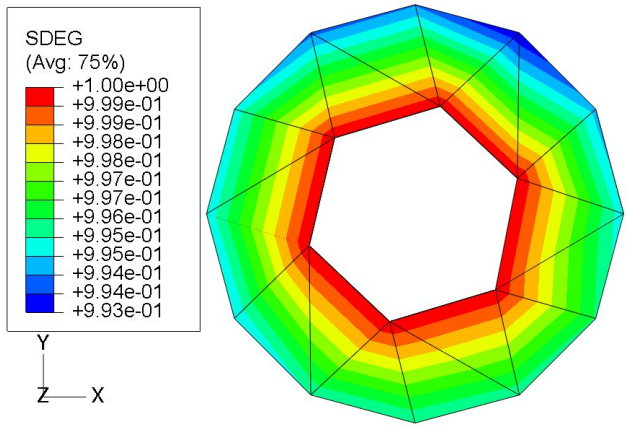

(b) ε=1.83%

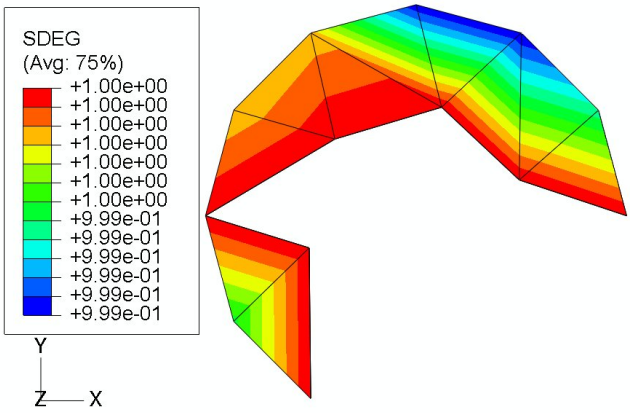

(c) ε=1.89%

Fig. 7 Evolution of damage variable SDEG for homogeneous cohesive elements model

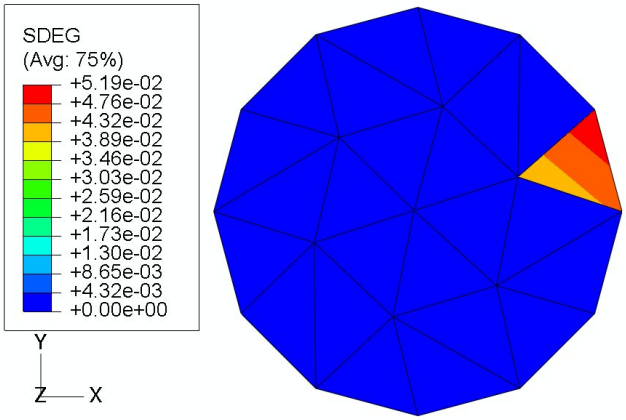

(a) ε=0.87%

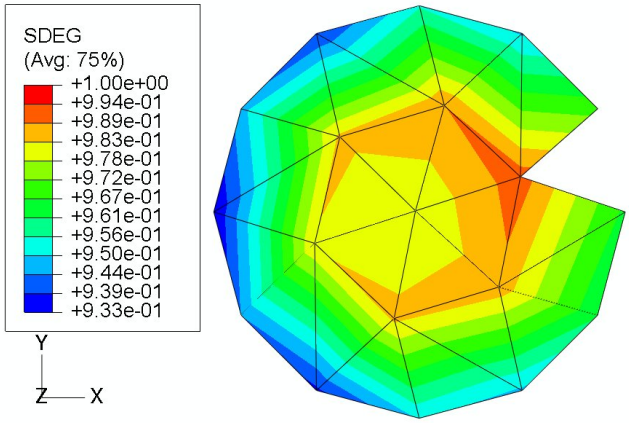

(b) ε=1.71%

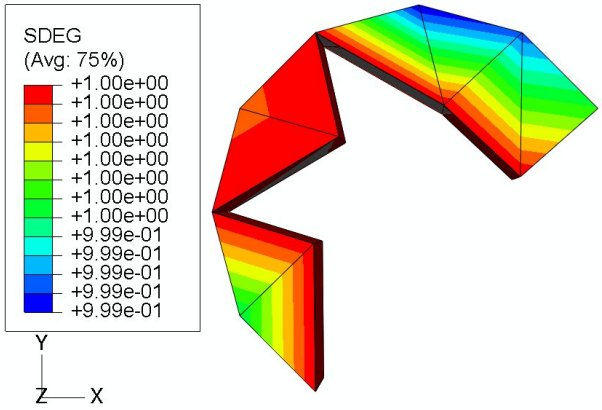

(c) ε=1.89%

Fig. 8 Evolution of damage variable SDEG for inhomogeneous cohesive elements model

As expected, the damage initiation occurs at the weakest element and earlier for the case of the inhomogeneous cohesive elements model, than for the case of the homogeneous cohesive elements model (Fig. 7-8). The fiber breaks at the same time (with strain equal 1.92%). From Fig. 9 and Fig.10, one can see that the stress-strain curves and strain energy-strain curves are very similar. However, it is notable that the damage begins in the center, near the axis of the fiber in the case of the ideally homogeneous fiber strength properties. In the case of inhomogeneous fiber strength properties, the cracking in the fiber starts near the interface. Thus, while neglecting the local heterogeneity of fiber properties does not lead to large errors in estimating the global behaviour of composites, it does lead to a wrong picture of the damage evolution in the multiphase material.

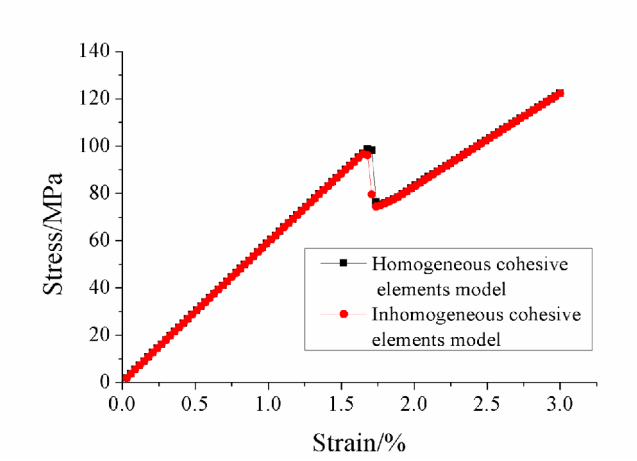

Fig. 9 Nominal stress-strain curve of the cell models with different modelling

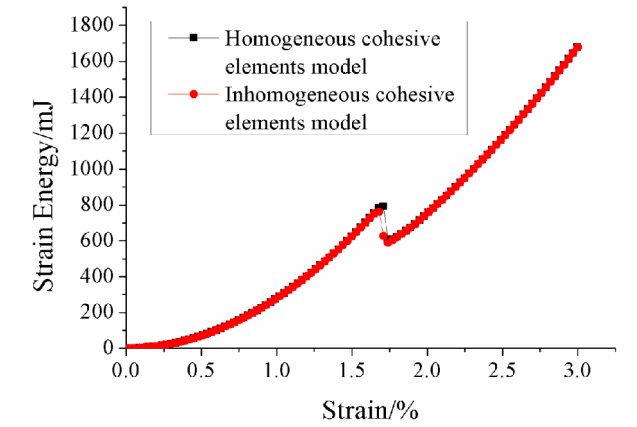

Fig. 10 Strain energy-strain curve of the cell models with different modelling

4.2 Single fiber unit cell with damageable interface: comparison of damage modeling methods

A single-fiber FE microstructural model with interface (interphase) layer is shown in Fig. 1(b). In the framework of the damageable layer model, the interface was taken as a layer with finite thickness, made from a third material, with averaged properties of the fiber and matrix. The Young modulus of interface material was assumed to 37.9GPa (the average value of the Young modulus of fiber and that of the matrix) and Poisson's ratio 0.37 (the Poisson's ratio of the matrix). According to [22], the interfacial shear strength between the fiber and the matrix is around 27 MPa. In this section, the values of fiber strength 1000 MPa and interfacial shear strength 30MPa are used.

Further, a single fiber unit cell model with damageable interface was generated using the cohesive elements. The three-dimensional 8-node linear brick cohesive elements COH3D8 were introduced in the interface layer. Similarly to the cohesive elements in fibers, the stiffness of the cohesive elements in interface was calculated as Young modulus divided by the thickness of cohesive element, and was 180 GPa. The maximum nominal stress traction-interaction failure criterion was selected for the damage initiation in the cohesive elements, and the energy-based

damage evolution law is selected for damage propagation. The damage initiation stress was 30MPa. Fracture energy in the interface was calculated with the use of Eqn. (1).

The stress-strain curves of the two cell models are shown in Fig. 11. One can see that the fiber breakage is observed in the cohesive model at slightly higher load, than in the damageable layer model. The reason is that while the elements in the damageable layer lose their stiffness stepwise, the stiffness lost by the cohesive elements is a monotonous function of strain.

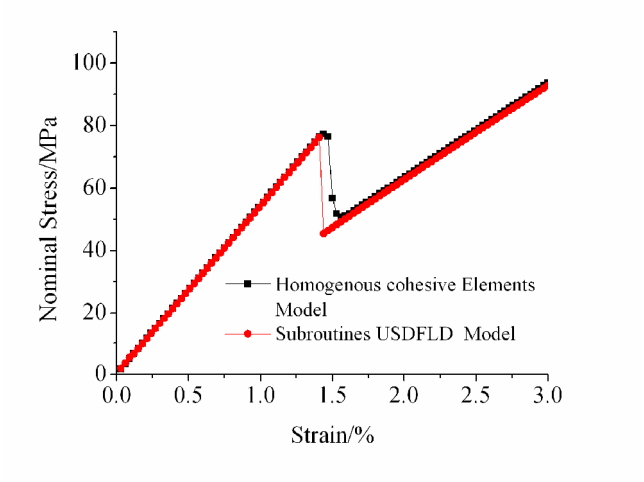

Fig.11 Stress-strain curve of the cell model

In order to see the process of damage evolution, the evolution of damage variable SDEG in the two damageable parts is shown in Fig. 12. It can be seen that the fiber cracking begins earlier than the interface damage, though the strength of fiber (1000MPa) is much higher than that of interface (30MPa). After the fiber is broken, the interface is getting damaged rapidly.

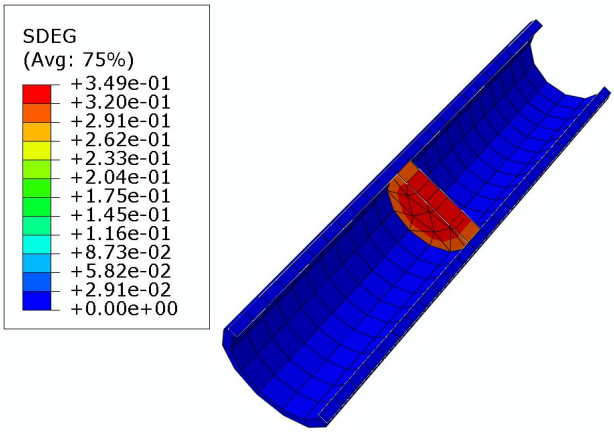

(a) ε= 1.44%

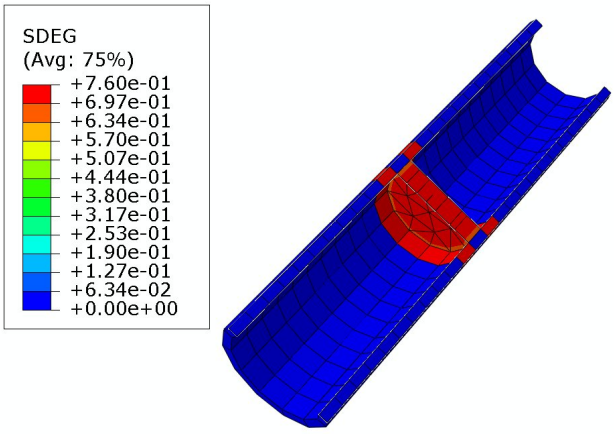

(b) ε=1.47%

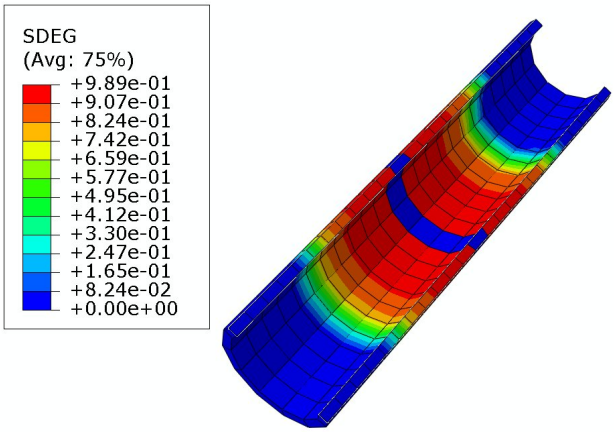

(a) ε= 1.50%

Fig. 12 Evolution of damage variable SDEG for all cohesive elements

4.2.2 Effect of interface and fiber strengths on the effective response of the composite cell

In order to study the competition between the two damage parts in composites (interface damage and fiber fracture), two series of simulations were carried out.

In the first series of simulations, the strength of interface layer was varied, while the strength of fiber was assumed to be constant. Several levels of the critical stress of interface layer have been taken: 100, 200, 300 and 400MPa. The strength of the fiber was 900MPa. The nominal stress-strain curves of the cells model in this case are shown in Fig. 13.

In the second series of simulations, the strength of fibers was varied, while the strength of interface layer was kept constant. Several levels of the critical stress of fiber have been taken: 600, 700, 800, 900 and 1000 MPa. The interface strength was 300MPa. The nominal stress-strain curves of the cell models in this case are shown in Fig. 14.

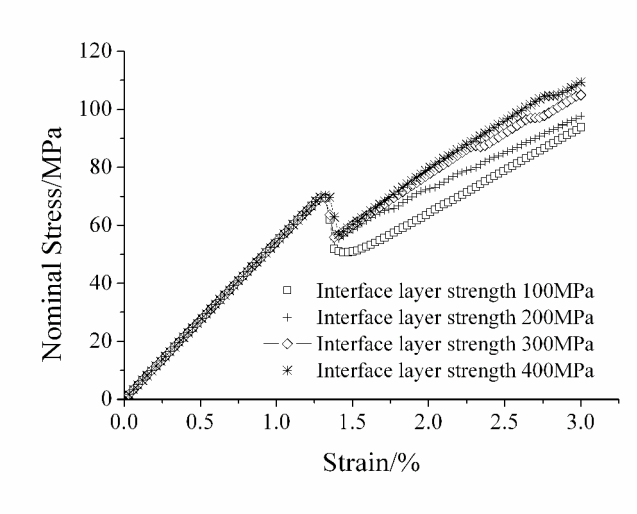

Fig. 13 Nominal stress-strain curve of the cell models (with different interface layer strength)

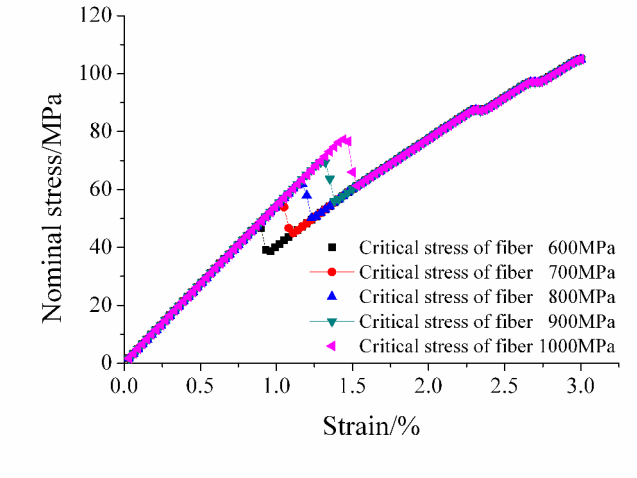

Fig. 14 Nominal stress-strain curve of the cell models (with different fiber critical stress)

From Figure 13 can be seen that the interface layer strength has no effect on the effective response of the composite with intact fibers. However, after the fiber is broken, the stiffness of the composite is the higher, the higher interface layer strength.

4.2.3 Inhomogeneous cohesive elements in the interface layer

Let us consider the effect of the inhomogeneity and variability of the local interface properties on the strength of composite. In order to study the effect of the variability of local interface properties, we introduced various cohesive elements in the interface layer of the single fiber unit cell. 288 cohesive elements (with correspondingly 288 various material properties, with random strengths) were placed in the interface layer. The strengths of interface elements were varied randomly from 100MPa to 200MPa, according to the uniform probability distribution law.

Figure 15 shows the nominal stress-strain curves of the unit cell models with cohesive elements with constant and randomly varied properties in interface layer.

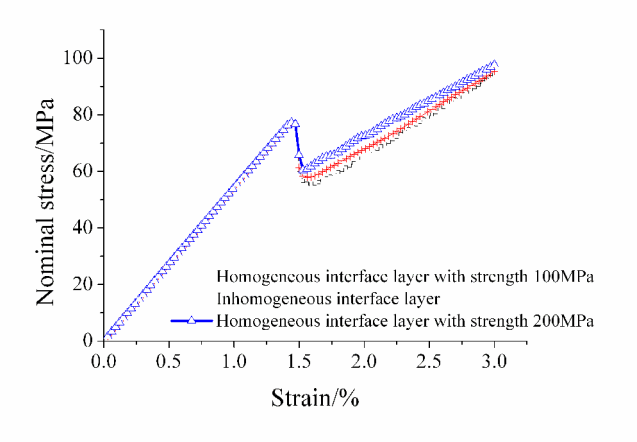

Fig. 15 Stress-strain curves for homogeneous and inhomogeneous interface layers.

One can see from Figure 15 that the effective response of the model with the interface layer with random varied local properties is just between the corresponding curves for the cases of constant strengths of interfaces. One can conclude that the variability of local interface properties does not have any special effect on the composite strength, apart from the effect of the averaged interface strength. Thus, it is enough to take into account the averaged interface strength, and not its variability, in the damage simulations of composites. However, this conclusion was tested only for tensile loading along the fiber axes; most probably, it can be generalized for shear or compressive loading of composites.

4.3 Competition among different damage modes in composites

In this section, we seek to consider the interaction among all three damage modes in composites (matrix cracks, fiber/matrix interface damage and fiber fracture), and the sequence of damageable evolution.

4.3.1 Single fiber model with one matrix crack and homogeneous interface layer

A single-fiber FE cell model with cracked fiber, damaged interface matrix/fiber interface and one matrix crack is shown in Fig. 1(c). Additionally to the single fiber model with damageable interface considered above, this model allows the damage and cracking on matrix. Three-dimensional 6-node linear triangular prism cohesive element COH3D6 was employed in the damageable layers in the fiber and matrix. Three-dimensional 8-node linear brick cohesive element COH3D8 was employed in fiber/matrix interface layer. Correspondingly, three cohesive materials with the following strengths were created: 600, 100 and 67 MPa (fiber fracture, interface and matrix crack, respectively). The displacement load in Z-direction is 0.135mm. The evolution of damage variable SDEG in the three damageable parts is shown in Fig. 16. The nominal stress-strain curve of the cell model is shown in Fig. 17.

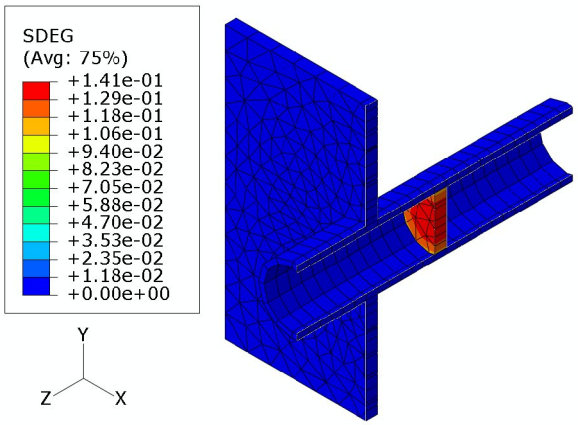

(a) ε=0.85%

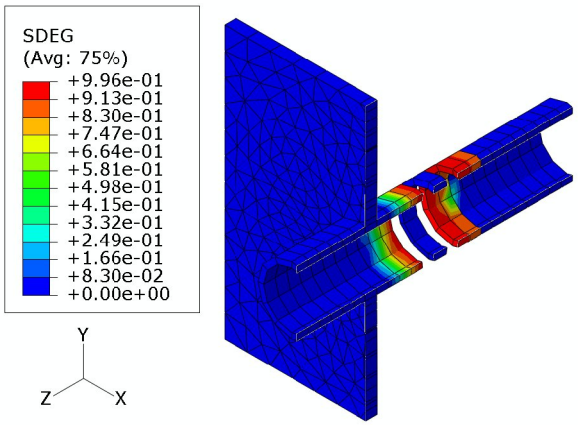

(b) ε=1.10%

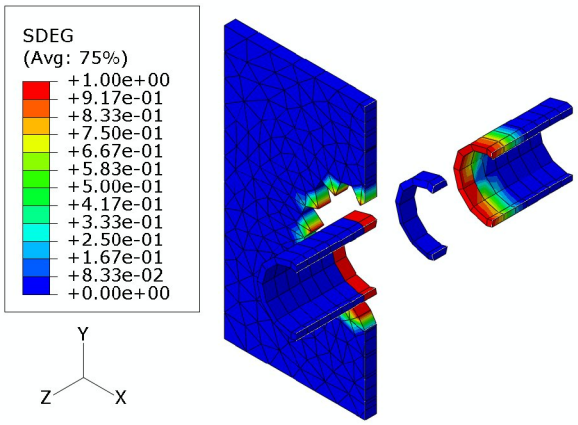

(c) ε=1.35%

Fig. 16 Evolution of damage variable SDEG of the model

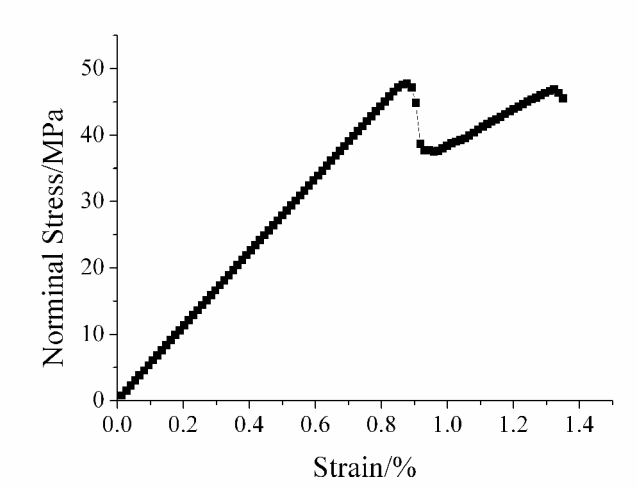

Fig. 17 Nominal stress-strain curve of the cell model

From Fig. 16, one can see that the sequence of damage evolution in this case is as follows: first, fiber cracking, then interface debonding, and, finally, the matrix crack damages at last. The stiffness of composites is drastically reduced after the fiber failure. The composite with the failed fiber deforms elastically, with the reduced Young moduli. Further reduction of the composite stiffness takes place when the matrix cracking begins.

4.3.2 Multiple matrix cracking

In this section, we consider the multiple cracking in the matrix and its interaction with interface debonding and fiber cracking. A single fiber unit cell model with three damageable layers in matrix (additionally to the damageable layers in the interface and fiber) is shown in Fig. 1(d).

The material properties were the same as in the previous model. The interface strengths were taken at two levels: 100MPa and 200MPa. Further, for the case of inhomogeneous interface, the randomly distributed strengths between 100MPa to 200MPa were assigned to the elements on the interface.

In the simulations, it was observed that the matrix crack, which is closest to the fiber fracture, begins to grow first, and the other two potentially damageable layers don't get damaged. The nominal stress-strain curves for different interface strengths are shown in Fig. 18.

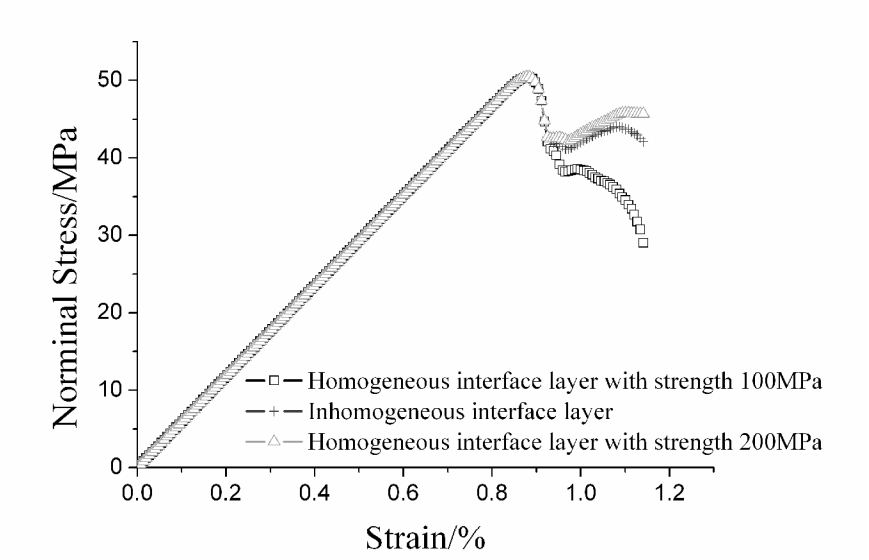

Fig. 18 Nominal stress-strain curve of the unit cell models with different interface properties

It can be seen from Fig. 18 that the matrix cracking strongly depends on the interfacial strength of composite: the higher the interfacial strength, the less matrix damage. Depending on the interface strength, the composite can keep rather high stiffness after the fiber failure (the case of the interface layer strength 200 MPa), or its stiffness will continue to fall (the interface layer strength 100 MPa). Thus, the high interfacial strength may compensate for the brittleness of matrix, and delay the matrix cracking in the composites.

Comparing Figures 15 and 18, one can state that the interface strength has a very weak influence on the composite behaviour in the case of strong, non-damageable matrix, and a very strong influence on the composite stiffness in the case of weaker, brittle matrix.

5. Single-fiber versus multi-fiber modelling: Effect of fiber crack interaction

In this section, we consider the effect of multiple fibers, interaction between many fiber cracks and other defects on the strength and damage evolution in composites.

5.1 Multifiber unit cell model: Cohesive elements versus damageable layer model

Let us consider the effect of multiple fibers on the damage evolution in the composite. 10-fiber unit cell model, generated by the program code "Meso3DFiber" [1-3] is shown in Fig.1 (e). Every fiber in the cell has one damageable layer, randomly placed along the fiber axis. The volume content of fibers was taken 34%. The fiber strength distribution follows Weibull probability law with parameters σ_0=929.8MPa and m=2.55 [22]. The boundary conditions were described in section 3. Two modelling methods, damageable layer model and cohesive elements modelling, were employed to study the damage evolution.

The nominal stress-strain curves of the cell model are shown in Fig. 19. In this model, only fibers are considered to be damageable. The matrix and interface are supposed to be very strong and non-damageable.

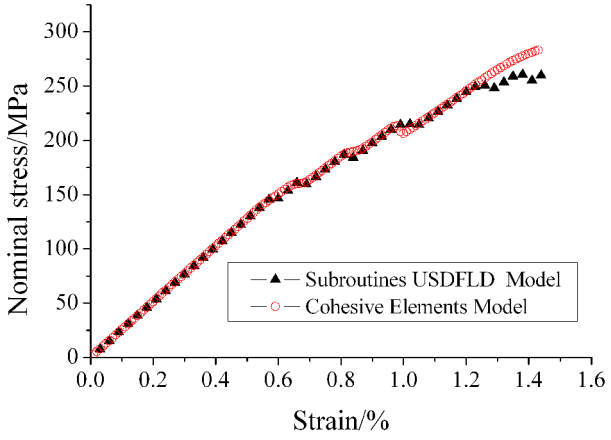

Fig. 19 Nominal stress-strain curve of the cell models with different modelling

Comparing Figures 3 and 19, one can see that the model is more sensitive to the method used in the case of multifiber cell, than in the case of single the fiber unit cell. As expected, the stress-strain curve in the case of multifiber model has a zigzagged shape.

5.2 Effect of multiple fiber cracking

In this subsection, we seek to study the effect of multiple fiber cracking on the strength and damage evolution in composites. We used 10-fiber unit cell model, similar to that as shown in Fig. 1(f). However, two (not one) damageable layers were placed in every fiber. The locations of both damageable sections were determined using the random number generator. From totally 20 damageable layers in 10 fibers, each damageable layer was assigned its own strength, following the Weibull probability law with parameters σ_0=929.8MPa and m=2.55.

The nominal stress-strain curves of the multifiber unit cell models with one and two damageable layers were shown in Fig. 20.

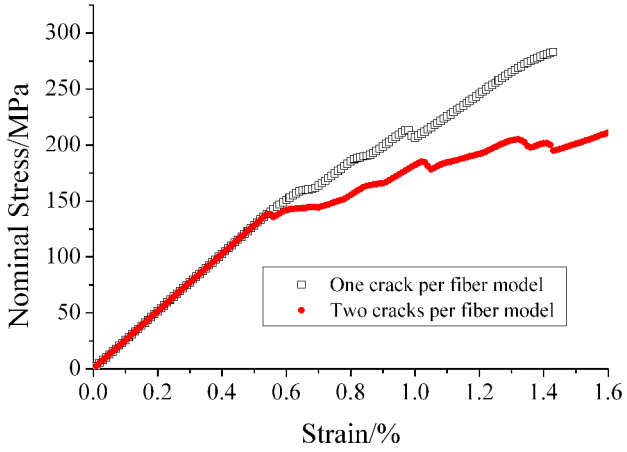

Fig. 20 Nominal stress-strain curves of the multifiber unit cell models with one and two damageable layers per fiber

One can see from Fig. 20 that the possibility of multiple cracking of fibers does influence the stiffness and damage growth in composites (as different from the possibility of multiple cracking in matrix!). The loss of stiffness due to the multiple fiber cracking is much bigger than that due to the single fiber cracking.

Figures 21 shows the stress-strain curves together with the damage strain curves. The damage is calculated as an amount of failed finite elements in fibers. One can see that the zigzags on the stress-strain curve correspond to the fiber cracking events.

Figure 22 gives the maximum principal (or Mises) stress distributions before and after the second cracking in a fiber. The stresses are highest in the matrix regions between two neighbouring fiber cracks. One can see from the Figures 22a and 22b, that the second cracking in an already cracked fiber takes place rather closely to, and in the area of high stress concentration of a crack in another, adjacent fiber. Thus, the cracks in the fibers can induce the cracking in neighbouring fibers.

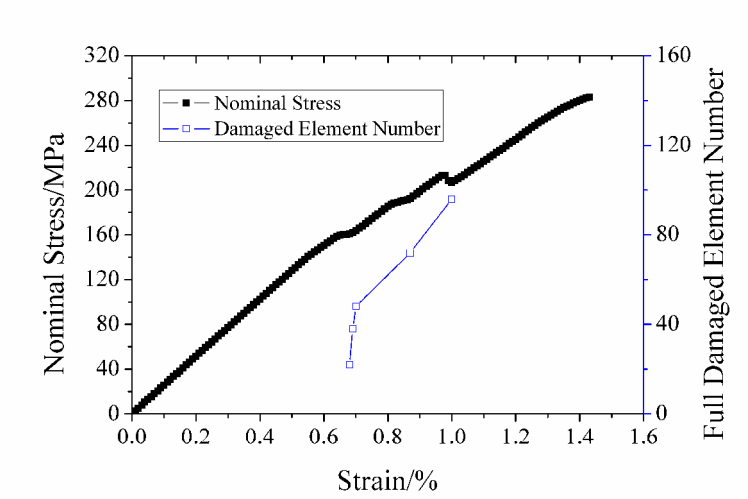

(a) One crack per fiber model

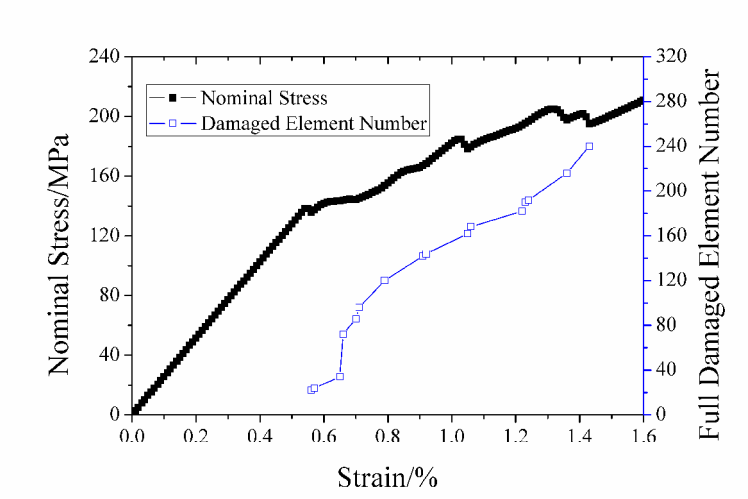

(b) Two cracks per fiber model

Fig. 21 Nominal stress and fully damaged element number versus strain curves of the two models

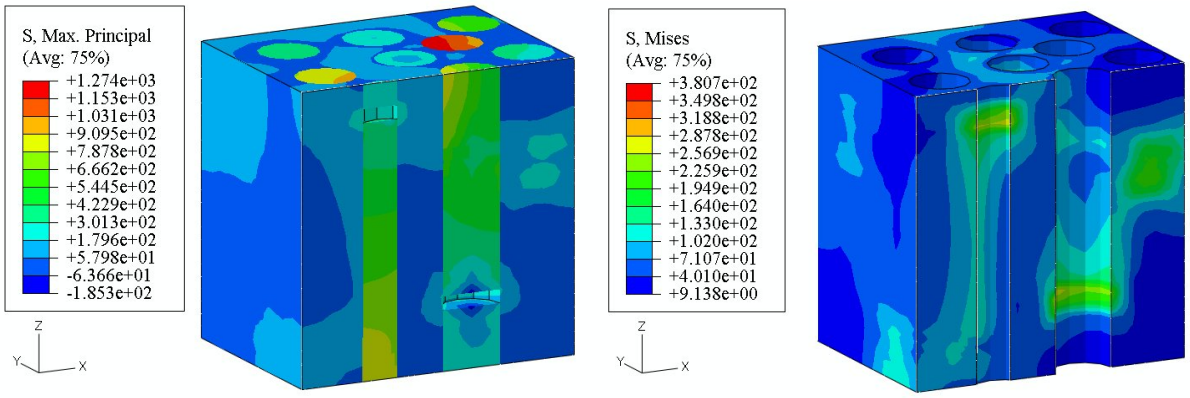

(a)Before the second crack in a fiber ε=1.41% (with and remove fibers)

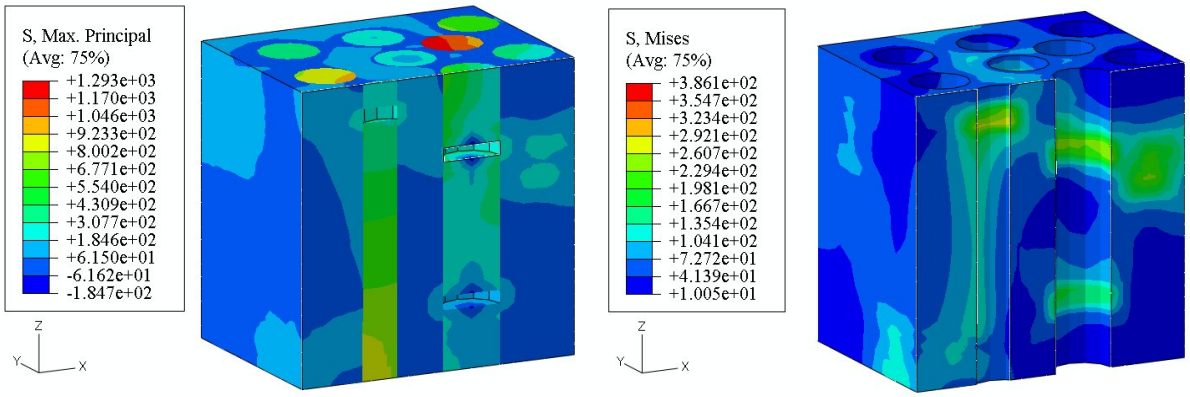

(b) After the second crack in the fiber ε=1.43% (with and remove fibers)

Fig.22 Max principal stress distribution before and after the second crack in one fiber full damaged

6. Conclusion

In this study, the simulations of damage evolution in fiber reinforced composites, based on different modelling techniques and seeking to clarify the effects of interface strength, interface homogeneity, interaction between cracks in different phases on the strength and damage evolution in the composites.

The computational investigations lead us to the following conclusions.

- In the considered material, the sequence of damage evolution can be described as follows: first, fiber cracking, then interface debonding, and, finally, the matrix crack damages at last. The fiber cracking begins earlier than the interface damage, though the strength of fiber is much higher than that of interface. After the fiber is broken, the interface is getting damaged rapidly. The stiffness of composites is drastically reduced after the fiber failure. The composite with the failed fiber deforms elastically, with the reduced Young moduli. Further reduction of the composite stiffness takes place when the matrix cracking begins.

- The strength of the interface layer has no effect on the effective response of the composite under tensile loading before the fibers begin to crack. However, after the fiber is broken, the stiffness of the composite is the higher, the higher interface layer strength.
- The variability of local interface properties does not have any special effect on the tensile strength of composites, apart from the effect of the averaged interface strength. It is therefore enough to take into account the averaged interface strength, and not its variability, in the damage simulations of composites.
- The matrix cracking strongly depends on the interfacial strength of composite: the higher the interfacial strength, the less matrix damage. Depending on the interface strength, the composite can keep rather high stiffness after the fiber failure, or its stiffness will continue to fall. Thus, the high interfacial strength may compensate for the brittleness of matrix, and delay the matrix cracking in the composites. The interface strength has a very weak influence on the composite behaviour in the case of strong, non-damageable matrix, and a very strong influence on the composite stiffness in the case of weaker, brittle matrix.
- It was observed in the simulations that the second cracking in an already cracked fiber takes place rather closely to, and in the area of high stress concentration of a crack in another, adjacent fiber. Thus, the cracks in the fibers can induce the cracking in neighbouring fibers.

As differed from single fiber unit cells, the multifiber cells allows to take into account the interaction between competing damage mechanisms, multiple fiber breaks, etc. The study of damage evolution in multi-fiber models is to be continued in the forthcoming works.

Acknowledgements:

This work was supported by the Commission of the European Communities through the Sixth Framework Program Grant UpWind.TTC (Contract No. SES6-019945). This support is greatly acknowledged. The main part of the research described in this paper was carried out during the first author's research stay at AFM, Risø.DTU. The first author would like to express his thanks to Professor Dr. Dorte Juul Jensen, Drs. Bent F. Sørensen, Xiaoxu Huang, Stergios Goutianos and Hai Qing for their help and fruitful discussions. Special thanks also go to Ms. Jiang Shuqin for her help in improving the manuscript.

References:

[1] L. Mishnaevsky Jr., Computational Mesomechanics of Composites, John Wiley and Sons, London, 2007.

[2] L. Mishnaevsky Jr., P. Brøndsted, Micromechanisms of damage in unidirectional fiber reinforced composites with polymer matrix: 3D computational analysis, in preparation

[3] L. Mishnaevsky Jr., P. Brøndsted, 3D numerical modelling of damage initiation in unidirectional fiber reinforced composites with ductile matrix, Mater. Sci. Eng. A, Accepted, doi:10.1016/j.msea.2007.09.105

[4] A.M. Sastry, S.L. Phoenix, J. Mater. Sci. Lett., 12(1993)1596.

[5] C.M.Landis, I.J. Beyerlein, R. M. McMeeking, J. Mech. Phys. Solids, 48(2000)621.

[6] I.J.Beyerlein, S.L. Phoenix, J. Mech. Phys. Solids, 44(1996)1997.

[7] Z. Xia, W. A. Curtin, T. Okabe, Compos. Sci. Technol., 62(2002)1279.
[8] F. Kun, S. Zapperi, H.J. Herrmann, Eur. Phys. J. B, 17(2000)269.
[9] F.Raischel, F. Kun, H.J. Herrmann, Phys. Rev. E, 73(2006) 66101.
[10] D.B. Marshall, B.N. Cox, A.G. Evans, Acta Metall., 33(1985)2013.
[11] L.N. McCartney, Proc. R. Soc. Lond. A, Math. Phys. Sci., 409(1987)329.
[12] W.S. Slaughter, Int. J. Solids Struct., 30(1993)385.
[13] L. Mishnaevsky Jr., S. Schmauder, Appl. Mech. Rev., 54(2001)49.
[14] D. Ouinas, B. Serier, B.B. Bouiadjra, Comput. Mater. Sci., 39(2007)782.
[15] M.R. Kabir, W. Lutz, K. Zhu, S. Schmauder, Comput. Mater. Sci.,36(2006)361.
[16] G.I. Giannopoulos, D. Karagiannis, N.K. Anifantis, Comput. Mater. Sci., 39(2007)437.
[17] T. Rahman, W. Lutz, R. Finn, S. Schmauder, S. Aicher, Comput. Mater. Sci., 39(2007)65.
[18] K. Zhu, S. Schmauder, Comput. Mater. Sci., 28(2003)743.
[19] S. Feih, A. Thraner, H. Lilholt, J. Mater. Sci., 40(2005)1615.
[20] G. Debotton, L. Tevet-Deree, J. Compos. Mater., 38(2004)1255.
[21] J. M. L. dos Reis, Mater. Res., 8(2005)357.
[22] G. KBV Kumar, Studying the influence of glass fiber sizing roughness and thickness with the single fiber fragmentation test. Kristianstad University, Degree Project, 2006.
[23] C. Gonzalez, J. LLorca, Acta Mater., 54(2006)4171.
[24] L. Mishnaevsky Jr., Compos. Sci. Technol., 66 (2006)1873.
[25] L. Mishnaevsky Jr., Mater. Sci. Eng. A, 407(2005)11.